Optical Engineering

OpticalEngineering.SPIEDigitalLibrary.org

Identification of substances from diffuse reflectance spectra of a broadband quantum cascade laser using Kramers–Kronig relations

Igor L. Fufurin
Anastasiia S. Tabalina
Andrey N. Morozov
Igor S. Golyak
Sergey I. Svetlichnyi
Dmitry R. Anfimov
Igor V. Kochikov

Igor L. Fufurin, Anastasiia S. Tabalina, Andrey N. Morozov, Igor S. Golyak, Sergey I. Svetlichnyi, Dmitry R. Anfimov, Igor V. Kochikov, "Identification of substances from diffuse reflectance spectra of a broadband quantum cascade laser using Kramers–Kronig relations," *Opt. Eng.* **59**(6), 061621 (2020), doi: 10.1117/1.OE.59.6.061621

Identification of substances from diffuse reflectance spectra of a broadband quantum cascade laser using Kramers–Kronig relations

Igor L. Fufurin,[a],[*] Anastasiia S. Tabalina,[a] Andrey N. Morozov,[a] Igor S. Golyak,[a] Sergey I. Svetlichnyi,[b] Dmitry R. Anfimov,[a] and Igor V. Kochikov[c]
[a]Bauman Moscow State Technical University, Moscow, Russia
[b]Russian Academy of Sciences, Chernogolovka Branch of the N.N. Semenov Federal Research Center for Chemical Physics, Chernogolovka, Russia
[c]M.V. Lomonosov Moscow State University, Research Computer Center, Moscow, Russia

Abstract. A real-time automated system for remote substance identification on various surfaces without preliminary sample preparation is presented. In practice, it can be used, for example, as an alerting system to signal the presence of some contaminants. The main components of the system are diffuse reflectance spectra acquisition module, data processing module, and identification module. Development of each module was based on the choice of appropriate devices and algorithms, either existing or newly designed. The experimental setup consists of a quantum cascade laser emitting in the spectral range of 5.3 to 12.8 μm with a HgCdTe photodetector. To achieve better selectivity of substance recognition, identification algorithms were based on the absorption and transmission spectra calculated from the recorded diffuse reflectance spectra. Spectra conversion algorithms employed Kramers–Kronig relations, phase spectra extrapolation, and phase correction. The system was supplied with the recognition database composed of certain commercially available substances. The experiments showed that the usage of transmittance spectra significantly improved the sensitivity of the identification method; the remote identification limit of 30 μg acetylsalicylic acid has been experimentally confirmed. For similar substances, such limit was estimated as 10 $\mu g/cm^2$ at a distance of 1 m. © *2020 Society of Photo-Optical Instrumentation Engineers (SPIE)* [DOI: 10.1117/1.OE.59.6.061621]

Keywords: spectroscopy; identification; remote sensing; quantum cascade laser; Kramers–Kronig relations.

Paper 191494SS received Oct. 25, 2019; accepted for publication Jan. 14, 2020; published online Feb. 8, 2020.

1 Introduction

The identification of chemical substances is an essential task in many fundamental and applied areas of research. Methods of studying the chemical composition of substances are largely determined by physicomechanical characteristics of the test substance and by measurement conditions.[1–4] Optical spectroscopy is widely used for the analysis of the composition and structure of substances in laboratory and field tests.[5,6] The most common methods of optical spectroscopy are Fourier transform infrared (FTIR) spectroscopy,[7,8] nondispersive infrared (NDIR) spectroscopy,[9] and Raman spectroscopy.[10,11] In addition, there are methods of substance analysis using terahertz radiation[12] and photoluminescence methods.[13]

FTIR and NDIR spectroscopy are time-tested routine methods for the analysis of substances in the gaseous phase and are widely used in field conditions.[14–16] Methods of passive FTIR spectroscopy allow identifying gases in the atmosphere at a distance of several kilometers.[17,18]

---

[*] Address all correspondence to Igor L. Fufurin, E-mail: igfil@mail.ru

Due to the significant absorption coefficients, the analysis of liquid and crystalline compounds by methods of infrared absorption spectroscopy requires sample preparation and is carried out only in laboratory conditions.

For field studies of substances in the liquid and solid phase, Raman spectroscopy is widely used.[19,20] This method is characterized by high selectivity and sensitivity; it allows identifying substances in optically transparent packages without sampling. A significant drawback of this method is the small quantum efficiency of the Raman scattering, as well as the high level of intrinsic fluorescence for some substances, and the need to use sufficiently powerful sources of exciting radiation.

Since the middle of the 20th century, analysis of diffusely reflected radiation was used to study the chemical composition of substances[21–25] based on the broadband infrared sources and monochromators and (later) on Fourier spectrometers. Recently, there has been significant progress in laser technologies related to the development of quantum cascade lasers (QCLs). Modern QCLs can generate laser radiation with a tuning range of up to 1000 cm^{-1} in the mid-IR range with a pulsed power of more than 100 mW and a physical laser chip size less than an inch. The use of QCLs and sensitive IR photodetectors enables the creation of portable spectrometers capable of recording the spectra of diffusely reflected IR radiation.[22] The method suggested in Refs. 26 and 27 allows identifying substances in solid and liquid phases in laboratory or field conditions without taking samples. The method has a number of critical advantages, such as the possibility of remote-sensing analysis on natural surfaces in real time, immunity to external illumination, safety for both the researcher and the test sample, and the possibility to form a wide beam of probe radiation for surface scanning. In laboratory conditions, the proposed method can complement the attenuated total reflectance (ATR) spectroscopy and diffuse reflectance infrared Fourier transform (DRIFT) spectroscopy[28]; in field conditions, the method can complement Raman spectroscopy.

However, it is important to note that diffuse reflectance spectra have relatively low selectivity. The use of the Kramers–Kronig integral relations, which connect the real and imaginary parts of an electromagnetic wave taking into account the Fresnel equations, allows reconstructing the absorption spectrum of the test sample based on the experimentally recorded diffusely reflectance spectrum.[21,23] Further detection and identification of substances can be conducted using the calculated absorption or transmittance spectra, which significantly increases the identification reliability in many cases.

This paper presents a real-time automated system for remote substance identification on various surfaces without preliminary sample preparation. In practice, it can be used, for example, as an alerting system to signal the presence of some contaminants. The system is not regarded as a precise analytical tool; its main goal is supporting fast remote measurements under field conditions. The main components of the system are diffuse reflectance spectra acquisition module, data processing module, and identification module. The development of each module was based on the choice of appropriate devices and algorithms either existing or newly designed.

The system consists of the experimental setup for recording diffuse reflectance spectra, the data processing module for converting them into absorption spectra, and the identification module using the database of transmittance spectra. The experimental setup for measuring diffusely reflected infrared radiation of solids and liquids on different surfaces consists of a QCL and a HgCdTe photodetector (MCT) cooled using a cascade of Peltier cells. The laser emits radiation in the spectral range of 5.3 to 12.8 μm with a peak power of 150 mW and a pulse duration of about 50 ns. The details of the experimental setup are given in Sec. 2.

To achieve better selectivity of substance recognition, identification algorithms were based on the absorption and transmission spectra generated from the recorded diffuse reflectance spectra. Spectra conversion algorithms employed Kramers–Kronig relations, phase spectra extrapolation and phase correction; these algorithms are considered in Sec. 3.

Due to the approximate nature of the spectra conversion methods, their applicability was verified on the set of real substances. The applicability and accuracy of the proposed method for the transformation of the optical coefficients have been verified by the simulations with the model substances representing an ensemble of damped harmonic oscillators (Sec. 4).

Using the identification methods,[15] we formulated an algorithm for substance identification on the basis of diffuse reflectance spectra.

Practical testing of the identification system was performed with the use of a database with multiple substances (Sec. 5). It has been shown that using absorption and transmittance spectra provides better selectivity than diffuse reflectance spectra and allows to enhance the sensitivity of the identification method. The combination of the known and newly suggested methods in the framework of a single system allowed to suggest a new powerful approach to remote substance detection and identification. We have experimentally proven the possibility of remote identification of 30 μg acetylsalicylic acid at 0.2-m distance. For similar substances, and with a certain upgrade of the system, we estimated the possible minimum detection threshold of about 10 $\mu\text{g}/\text{cm}^2$ at a distance about 1 m.

The tasks of this study are as follows:

- Development and creation of the experimental method and setup for recording diffusely reflectance IR spectra using a broadband QCL.
- Selection of appropriate existing and development of the new mathematical procedures for processing the reflectance spectra based on causality relations.
- Development of substance identification procedures based on the calculated absorption spectra and on the original reflectance spectra.
- Estimation of detection limits for the described identification method and technique.

2 Experimental Setup

Figure 1 shows the experimental setup used for recording diffuse reflectance spectra.

Infrared radiation from the QCL is incident normally on a nonreflecting substrate, where the test substance is located. For solids, the size of the particles is about 0.1 to 1.0 mm; for liquids, drop sizes are about 2 to 5 mm.

The laser emits in a pulsed mode with a peak power of up to 150 mW and the average power of about 20 mW. The pulse duration is about 50 ns, and a repetition frequency is about 1 MHz. The emitted radiation is in the spectral range of 5.3 to 12.8 μm with a tuning step of 2 cm^{-1}. The laser beam cross-section is about $2 \times 4\ \text{mm}^2$, the divergence is <5 mrad, and the power instability is ∼5%.

The test sample is located on a substrate 50 cm away from the laser. The infrared radiation falls on the sample and is reflected diffusely and/or specularly. The photodetector optics collect the reflected radiation at a certain angle within the solid angle of 40 deg on a sensitive area of a photodetector. The photodetector is a HgCdTe thermoelectrically cooled MCT photodetector

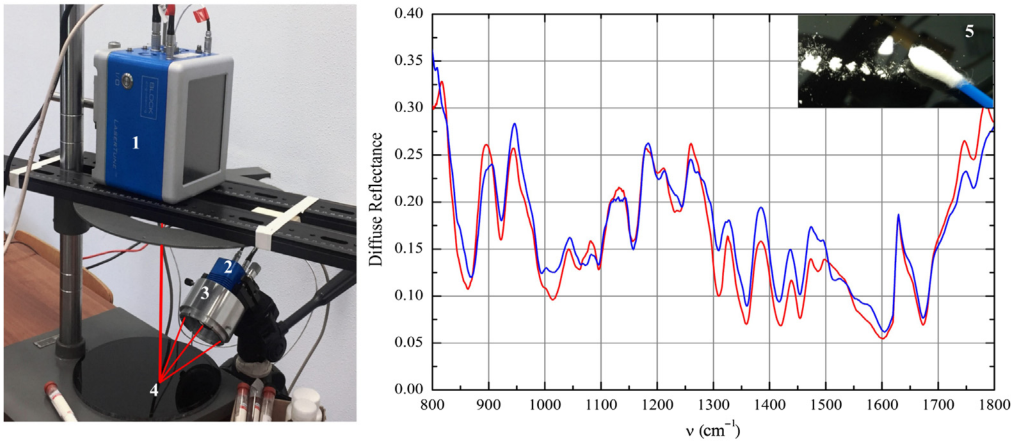

(a) (b)

Fig. 1 (a) Photo of the experimental setup for measuring diffusely reflected IR radiation spectra of substances in solid and liquid phases. Position 1, QCL (Laser Tune, Block Engineering, United States); position 2, MCT photodetector cooled by a cascade of Peltier cells; position 3, collecting optics of the detector; position 4, test sample on a nonreflecting substrate. (b) Typical forms of the measured spectra for 5 mg tryptophan. Position 5, picture of the test sample on the substrate.

(type Vigo PVMI-4TE) with a detectivity $D^* \sim 6 - 8 \times 10^9 \mathrm{cm\,Hz^{1/2}/W}$ and time resolution of at least 4 ns.

Signal-to-noise ratio (SNR) for laser emitted spectra is about 10^4 to 10^5. For tryptophan reflectance spectra [see Fig. 1(b)], SNR is about 45 to 50. The Pearson correlation coefficient for spectra in Fig. 1(b) is 0.97, which indicates good reproducibility of the measured spectra. The instability of the spectral lines' intensity is due to fluctuations of the laser power (about 5% for LaserTune QCL).

In the described setup, we first measured the radiation reflected from a golden plate to measure the spectral power of the incident radiation. Reflectivity of the plate in the working spectral range is no less than 98%. For further analysis, all reflectance spectra were normalized by the intensity of the incident radiation.

The influence of laser power fluctuations can be weakened by introducing a reference infrared channel for measuring the incident radiation power.

3 Theoretical Analysis: Data Processing Module

In many cases, the selectivity of the reflectance spectra is rather poor, leading to a low probability of correct identification of substances by infrared spectra. One of the methods to increase the reliability of substance identification is the numerical transformation of the reflectance spectrum to the absorption spectrum. The main aim of this section is showing that the absorption spectra may be obtained from diffuse reflectance spectra with reasonable accuracy. Spectral conversion has been verified by solving model problems.

3.1 *Application of the Causality Principle for the Transformation of the Optical Characteristics of a Test Substance*

In the case of a normal incidence of an electromagnetic wave at the interface between two media, according to Fresnel equations, algebraic relations take place for the reflection, refraction, and absorption coefficients. The reflectance of the medium can be represented as a complex function:

$$\hat{r}(\nu) = \frac{(n-1)+ik}{(n+1)+ik} = \eta e^{i\phi}, \tag{1}$$

where n is the refraction of the test substance, k is extinction, η is the amplitude of the reflected wave, and ϕ is the phase of the reflected wave.

Apparently, Eq. (1) written for the case of normal incidence of radiation on the interface between two media is oversimplified compared to the accurate theory of diffuse reflectance spectra. The use of this equation, however, may still be justified by assuming that there exists a model solid, whose optical characteristics match those of a real substance in the spectral region of interest.[25] The experimental setup has been designed to avoid registering specularly reflected radiation. The rest of registered input (diffuse reflection) comes from chaotically oriented surfaces of a substance (e.g., powder), and the input from different polarizations is effectively averaged. In this case, the registered data are independent of incident light polarization, and polarization-independent Eq. (1) is used to create an effective substance model.

Measured value is normalized reflectance defined as the square of the amplitude of the reflected wave $R(\nu) = \eta^2(\nu)$. By taking the logarithm of Eq. (1), we get $\ln[r(\nu)] = \ln[\eta(\nu)] + i\phi(\nu)$. Since reflectance in Eq. (1) must be causal, the amplitude $\eta(\nu)$ and phase $\phi(\nu)$ satisfy the Kramers–Kronig relations:[29]

$$\ln[\eta(\nu)] = V.p.\left(\frac{2}{\pi}\int_0^\infty \frac{\nu'\phi(\nu')}{\nu'^2-\nu^2}\mathrm{d}\nu'\right), \tag{2}$$

$$\phi(\nu) = V.p.\left(-\frac{2\nu}{\pi}\int_0^\infty \frac{\ln[\eta(\nu)]}{\nu'^2-\nu^2}\mathrm{d}\nu'\right), \tag{3}$$

where $V.p.$ means that the integrals are calculated as principal values.

Relations between the extinction, refraction, and amplitude of the reflected wave can be written as follows:

$$n(\nu) = \frac{1 - R(\nu)}{1 + R(\nu) + 2\sqrt{R(\nu)}\,\cos\,\phi(\nu)}; \quad k(\nu) = \frac{2\sqrt{R(\nu)}\,\sin\,\phi(\nu)}{1 + R(\nu) - 2\sqrt{R(\nu)}\,\cos\,\phi(\nu)}. \tag{4}$$

It is possible to acquire the extinction spectrum by measuring the reflectance spectrum. Conversion from extinction to absorption spectra can be implemented, as mentioned in Ref. 24. To calculate phase spectra using Kramers–Kronig relations, we need to calculate the integrals in the sense of the Cauchy principal value. In Ref. 30, the main methods for the numerical implementation of the Kramers–Kronig principle have been considered. Mostly, the methods come down to bypassing the singular point. In Ref. 31, the use of double Fourier transforms for causality relations has been proposed. This method has been chosen for implementation in the described real-time identification system due to its high computational efficiency.[23]

The most important problem in implementing the Kramers–Kronig relations for the spectrum $R(\nu)$ is that it is measured in the frequency range limited by the spectral range of the waves generated by QCL. In general, it is impossible to reconstruct complex spectral coefficient from the values of its real component in the limited frequency range. As a result, any algorithm of reconstructing the whole complex function has a semiempirical nature and therefore possesses only a limited applicability. The error of reconstructed characteristic should be estimated experimentally for a certain set of substances. Various approaches to approximate solution of this problem have been developed in earlier studies; two of them are applied in the present paper. The first approach is based on extrapolation of the measured spectra into the regions, where measurements are not available. This extrapolation affects the accuracy of calculating the phase and requires additional procedures of phase correction; these problems are discussed in Sec. 3. Another approach is creation of an effective model substance with the known analytical expressions for the real and imaginary parts of the studied optical coefficients; it is considered in Sec. 4. In both cases, the use of approximate reconstruction algorithms must be justified by independent measurements of the calculated characteristics.

3.2 *Extrapolation and Phase Correction*

Under real conditions, reflectance spectra are measured in a limited wavelength range ($5.3 - 12.8\ \mu$m in our case). As a result, the calculation of the absorption spectrum according to Eqs. (3)–(4) implies extrapolation of either the reflectance spectrum $R(\nu)$ or any spectrum associated with the reflectance spectrum with Kramers–Kronig relations. For the extrapolation of the experimental spectra,[24] the integral relations Eqs. (2) and (3) are converted to the following form:

$$\int_0^\infty \approx \int_0^{\nu_{\min}} + \int_{\nu_{\min}}^{\nu_{\max}} + \int_{\nu_{\max}}^{\nu_{\mathrm{ext}}}, \tag{5}$$

where $[\nu_{\min}, \nu_{\max}]$ is the frequency range where the experimental reflectance spectrum was measured, $\nu_{\mathrm{ext}} \gg \nu_{\max}$ is a sufficiently high maximum frequency to be determined empirically. The reflectance spectrum must be extrapolated to the regions $[0, \nu_{\min}]$ and $[\nu_{\max}, \nu_{\mathrm{ext}}]$. A review of methods for extrapolating the reflectance and phase spectra was presented in Refs. 23 and 24. In this work, we used exponential extrapolations functions:

$$R(\nu) = \begin{cases} R(\nu_{\min})\exp\left(\frac{\nu}{\nu_{\min}}\right)^{\alpha}, & \nu \in [0, \nu_{\min}] \\ R(\nu_{\max})\exp\left(\frac{\nu_{\max}}{\nu}\right)^{\beta}, & \nu \in [\nu_{\max}, \nu_{\mathrm{ext}}] \end{cases}. \tag{6}$$

The parameters of these functions have been determined empirically based on the measurements of absorption spectra and minimizing the difference between calculated and experimental spectra. For the set of test substances, the following values of parameters have been accepted, where $\alpha = 0.8$, $\beta = 2.7$, $\nu_{\min} = 810\ \mathrm{cm}^{-1}$, $\nu_{\max} = 1880\ \mathrm{cm}^{-1}$, and $\nu_{\mathrm{ext}} = 10000\ \mathrm{cm}^{-1}$.

In Refs. 32 and 33, it has been shown that the integral transformation Eq. (3) can be represented as follows:

$$\phi(\nu) = \frac{1}{\pi}\int_0^\infty \ln\left|\frac{\nu+\nu_0}{\nu-\nu_0}\right| \frac{d\,\ln[\eta(\nu)]}{d\nu}\mathrm{d}\nu. \tag{7}$$

The relation Eq. (7) shows that the contribution to the phase spectrum is insignificant for the spectral regions, where the amplitude of the reflected wave $\eta(\nu)$ changes slowly. The method of phase correction is based on constructing a baseline of the phase spectrum in the form of a low-order polynomial and subtracting the artifacts of the phase spectrum using Eq. (7). In the phase spectrum, which is calculated by Eq. (7), errors occur, such as negative values of phase angle and artifacts. They appear due to the limited spectral range and the presence of artifacts in the experimental reflectance spectrum. Negative values of phase angle cause negative values of extinction coefficient, and artifacts distort the calculated spectrum. We suggest using a phase correction algorithm based on constructing a baseline of the phase spectrum in the form of a low-order polynomial, which satisfies two basic requirements. First, the values of the phase angle must be positive after correction in the entire spectral range. Second, the values of the phase angle must tend to zero outside the basic spectral lines. It should be noted that constructing a baseline, in addition to eliminating obvious distortions in the spectrum, allows us to remove artifacts from the phase spectrum.

3.3 *Identification Technique*

Substance remote sensing and identification have been performed using a database of transmittance spectra calculated from reflectance spectra using Kramers–Kronig relations. To increase the SNR, we have used no less than 100 spectra for each substance. As a matching criterion, we have used the Pearson correlation of experimental and reference spectrum with the weight function $w(\nu)$ as in Eq. (8):

$$w(\nu) = \frac{I_0(\nu)}{\int_{\nu_{\min}}^{\nu_{\max}} I_0(\nu)\mathrm{d}\nu}. \tag{8}$$

The identification of substances consisted of a sequential comparison of the experimental spectrum and the spectra from the database. For each element of the database, the Pearson correlation coefficient with the experimental spectrum has been calculated. The substance from the database for which the correlation turned out to be the largest and exceeded the cutoff value is considered identified in this experiment. Often, cutoffs for the correlation coefficient are set for each substance separately. A detailed description of the identification algorithm has been given in Refs. 15 and 26.

3.4 *Spectra Conversion and Identification Algorithm*

Finally, an algorithm for substance identification can be described as follows:

1. Measuring reflectance $R(\nu)$ in the range $[\nu_{\min}, \nu_{\max}]$.
2. Extrapolation of $R(\nu)$ to the spectral regions $[0, \nu_{\min}]$ and $[\nu_{\max}, \nu_{\text{ext}}]$ according to Eq. (6).
3. Calculation of phase $\phi(\nu)$ using Eq. (3) and representing integrals as in Eq. (5).
4. Phase correction (removing phase artifacts appearing from extrapolation).
5. Calculation of extinction coefficient $k(\nu)$ from Eq. (4) and transmittance spectra.
6. Identification procedures using database of reference spectra.

4 Testing Spectra Conversion Approach Using Model Substance Spectra

To verify the applicability and efficiency of the described algorithm of spectra conversion, a set of model problems has been solved, and the reflectance and transmittance spectra have been calculated based on a certain model of a substance. In this section, we regard the Kramers–Kronig transformation as a semiempirical procedure, part of whose justification rests on the agreement between phases or optical constants obtained from the model with values measured more directly.[25]

Complex electric permittivity is represented by its real ε' and imaginary ε'' parts. Based on the Lorentz dispersion model, we treat a molecule as an ensemble of damped harmonic oscillations (DHO model):[34]

$$\varepsilon' = n_0^2 + \sum_j \frac{B_j(\omega_j^2 - \omega^2)}{(\omega_j^2 - \omega^2)^2 + \lambda_j^2\omega^2}, \quad \varepsilon'' = \sum_j \frac{B_j\lambda_j\omega}{(\omega_j^2 - \omega^2)^2 + \lambda_j^2\omega^2}, \tag{9}$$

where ω_j, B_j, and λ_j are the oscillator resonant frequency, the strength, and attenuation coefficient, respectively, for the j'th oscillator of the ensemble; n_0 is a constant.

The spectral indices of refraction n and extinction k can be obtained from the real and imaginary parts of the dielectric constant as follows:

$$n = \left\{\frac{1}{2}[(\varepsilon'^2 + \varepsilon''^2)^{1/2} + \varepsilon']\right\}^{1/2}, \quad k = \left\{\frac{1}{2}[(\varepsilon'^2 + \varepsilon''^2)^{1/2} - \varepsilon']\right\}^{1/2}. \tag{10}$$

Reflectance spectra have been calculated using Eq. (1). To provide closer resemblance of the model spectra to the real substances that will be tested in real applications, we have generated a model spectrum on the base of diethyl benzene-1,2-dicarboxylate [diethyl phthalate (DEP)]. DEP is similar to certain toxicants as regards physicochemical properties. Toxicants, in turn, are of interest for the express analysis of small quantities of a substance without preliminary sample preparation. Using the experimentally measured diffuse reflectance spectrum $R(\nu)$ of the drop of the test substance, the DHO model coefficients ω_j, B_j, and λ_j have been determined by the least square method in the range of 1050 to 1400 cm^{-1}. Table 1 presents the calculated values of the coefficients. The value of additive constant entering Eq. (9) is $n_0 = 2.71$.

To test the proposed method for calculating the spectral extinction coefficient from the reflectance spectrum using the Kramers–Kronig relations, we have conducted the following numerical experiment. For the ensemble of harmonic oscillators with parameters from Table 1 representing the model of liquid DEP, we have calculated the reflectance spectrum using Eqs. (1), (9), and (10) in the limited range of 1050 to 1400 cm^{-1} and applied the procedure described above to obtain the transmittance spectrum. Then, we have modeled the transmittance spectrum directly from Eq. (10) (Fig. 2 curve 2b) and calculate transmittance spectrum (Fig. 2 curve 1b) using Eqs. (2)–(4) from a modeled reflectance spectrum The correlation coefficient for the obtained transmission spectra for the same substance is 0.96, which confirms the reliability of the suggested method for converting optical characteristics.

Figure 2(a) shows the experimental (1a) and modeled (2a) diffuse reflection spectra. Figure 2(b) shows the calculated (1b) and modeled (2b) transmission spectra.

Table 1 Fitted DEP model parameters.

ω_j (cm^{-1})	$B_j \times 10^4$ (cm^{-2})	λ_j (cm^{-1})
807.46	308.31	157.36
1070.21	3.99	16.22
1114.15	12.37	33.41
1254.73	37.92	31.48

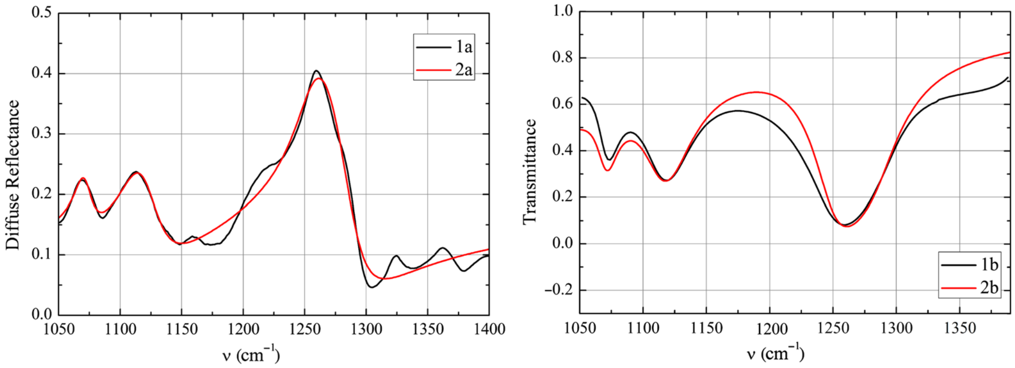

(a) (b)

Fig. 2 (a) Experimental and (b) modeled DEP spectral characteristics.

5 Results and Discussion

The final aim of the suggested algorithms is the identification of substances by spectra. Identification can either be done directly using the normalized reflectance spectra or using the calculated transmittance spectrum of the test substance based on the measured reflectance spectrum. For DEP, we will demonstrate the possibility of obtaining the transmittance spectrum for the measured reflectance spectrum and the possibility of identifying the substance from both the reflectance and transmittance spectra.

Figure 3(a) shows the experimental reflectance spectra (3a), the phase spectra calculated with and without correction, curves 2a and 1a, respectively. Figure 3(b) shows DEP transmittance spectra. Curve 1b is the calculated spectrum without phase correction; curve 2b is the calculated spectrum with a corrected phase; and curve 3b is the experimental transmittance spectrum. The extrapolation of the spectrum in the form of Eq. (6) was done in both cases. The correlation coefficient for the experimental transmittance spectrum and the calculated spectrum without phase correction is 0.78. Phase correction allows increasing the correlation between the experimental and calculated spectra to 0.89.

We have already mentioned that the selectivity of transmittance spectra is often better than that of reflectance spectra. This fact may be illustrated by the cross-correlation matrices for the databases of reflectance and transmission spectra shown in Figs. 4(a) and 4(b), respectively. Transmittance spectra have been obtained using the numerical algorithm described in this paper.

Figure 4(b) demonstrates that the matrix for the transmittance spectra is much closer to the diagonal form than the matrix for the reflectance spectra, Fig. 4(a). This fact indicates a greater selectivity of the transmittance spectra compared to reflectance spectra, which entails a better probability of correct detection of the investigated substances. This advantage of transmittance spectra also results in lower detection thresholds. As an illustration of the two methods, we have used the described experimental setup and the method for calculating the transmittance spectrum

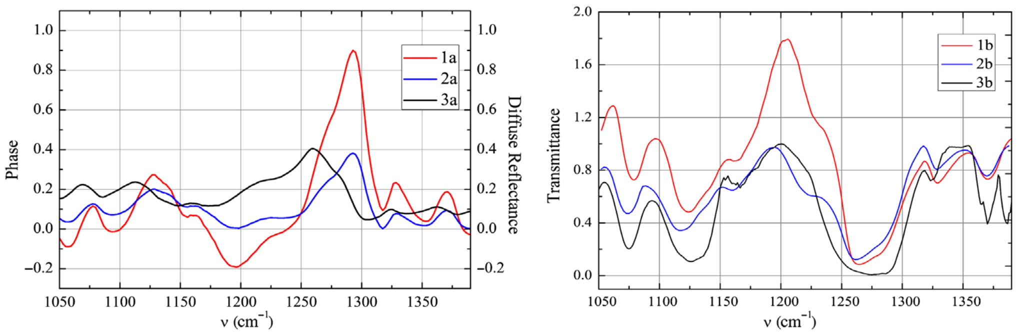

(a) (b)

Fig. 3 Phase correction procedures. (a), (b) Calculation of DEP transmittance spectra.

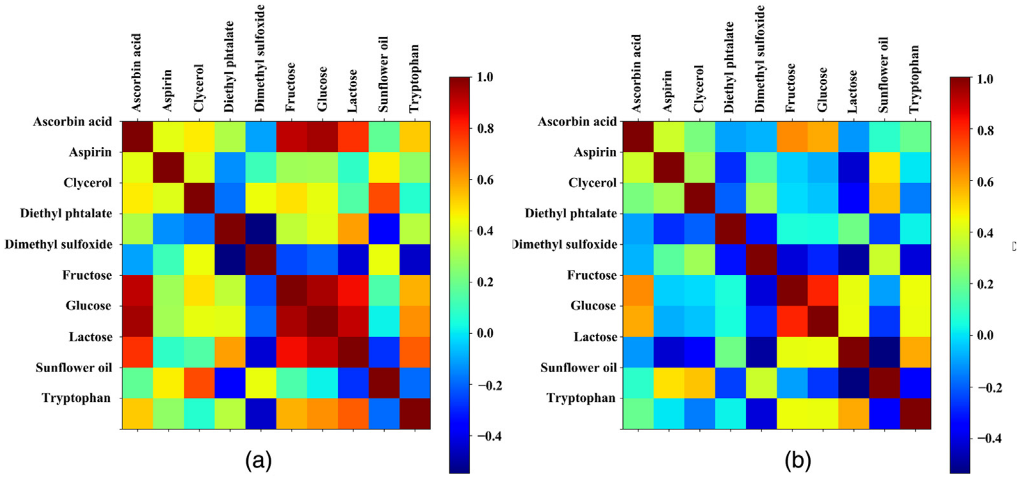

Fig. 4 (a, b) Cross-correlation matrices of the spectra database.

Table 2 Threshold sensitivity of the identification method.

	Using reflectance spectra		Using calculated transmittance spectra	
Test substances	Identification threshold (mg)	Pearson correlation	Identification threshold (mg)	Pearson correlation
Calcium chlorate	2.5	0.6	1.6	0.8
L-Tyrosine	0.75	0.9	0.04	0.6
Acetylsalicylic acid	6.38	0.9	0.03	0.5
Potassium chlorate	2.5	0.6	1.6	0.8

from the experimental reflectance spectrum to conduct an experiment on determining the minimum detectable amount of test substances. Table 2 presents the minimum detectable threshold values for several test substances.

The data in Table 2 were obtained when the spot of exciting laser radiation $2 \times 4\ \mathrm{mm}^2$ in size was completely filled with the test substance. The data in Table 3 show results for surface density of detected substances.

To test the described identification technique, we have performed remote sensing and identification of various substances on different backgrounds (see Table 4, where the symbol "—" means that we could not detect substance on that type of background).

Remote detection and correct identification of liquids and solids on different substances is a complicated task and a scope of a separate study. In this study, we have described a novel method for recording the diffusely reflected IR spectra using a broadband QCL and mathematical procedures for processing the reflectance spectra based on causality relations. The described method

Table 3 Detection limits for surface density.

Substance	Surface density (mg/cm^2)
Calcium chlorate	20
L-Tyrosine	0.50
Acetylsalicylic acid	0.33

Table 4 Probability of correct identification test substances on different backgrounds.

	Background			
Substance	Nonreflecting grass	Wood	Ceramics	Aluminum
Acetylsalicylic acid	0.86	0.69	0.4	—
Dimethyl sulfoxide	0.93	0.58	—	—
DEP	0.62	0.56	0.61	0.52
Glycerol	0.84	0.81	0.65	—
Sunflower oil	0.75	0.5	0.4	—
Tryptophan	0.90	0.87	0.72	0.55

and procedures enable remote detection and identification of liquids and solids on different substances. Data in Tables 2–4 show that the method can be used for substance identification in nonlaboratory conditions.

In the described experimental setup, the main factor that limits sensitivity and does not allow to achieve the theoretical detection limits is the instability of laser power. Power instability of about 5% significantly degrades spectra reproducibility [see Fig. 1(b)]. To reduce the influence of power instability, we suggest including a reference IR channel to the optical scheme and design of experimental setup (see Fig. 5).

We suggest using a QCL with peak power about 0.2 W, tuning range 7 to 11 μm and repetition frequency ~1 MHz; MCT photodetector with detectivity $D^* \sim 8 \times 10^9$ cm Hz$^{1/2}$/W, and 2×2 mm^2 size. Laser radiation on a beam splitter is divided into two parts: the first part goes directly to the reference detector and the second part via telescopic system falls on the test substance on the background, reflects from the test substance, and goes to the signal detector via telescopic and collecting optics. For the optical scheme, when laser radiation goes directly to photodetector, we can obtain the SNR in the range of 10^5 to 10^6. If we use accumulation of 100 spectra, we can obtain reflectance spectra with the SNR $\sim 10^4 \times \alpha$ for small distances from the test substance, where α is the reflection coefficient of the test substance. For test substances with scattering cross-section $\sigma \sim 10^{-19}$ cm^2 and molecular mass $m \sim 10^{-22}$ g, we can obtain reflectance spectra at a distance of $L \sim 1$ m with the SNR ~ 5. These estimates correspond to the possibility of remote detection and identification of test substance with a surface density of 10 μg/cm^2 at a distance 1 m.

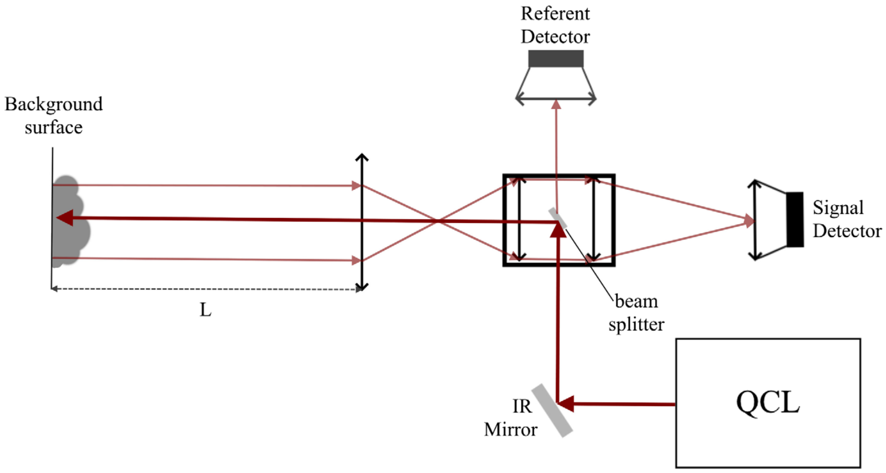

Fig. 5 Optical scheme of the upgraded experimental setup.

These estimates indicate that the described method of measuring and processing reflectance spectra is very promising for the real-time remote detection and identification of liquids and solids in small quantities on various backgrounds.

6 Conclusion

In this paper, we have described the construction, technical characteristics, and operating principle of the experimental setup for measuring the diffuse reflectance spectra of substances on different surfaces without preliminary preparation of samples. This setup is designed as an automated system for real-time substance identification.

Based on the Fresnel equation for the case of normal incidence of a wave on the interface between two media and the Kramers–Kronig relations for the real and imaginary parts of the complex refractive index, the numerical algorithm was suggested to extract the reflectance and extinction indices of a test substance from the measured diffuse reflection coefficient. The algorithm includes the methods of extrapolation and phase correction of the experimental spectra. The method for registering reflectance spectra and procedures of spectra processing and substance identification is a novel approach for remote detection and identification.

The applicability and efficiency of the suggested algorithm for spectra conversion and identification have been proven on the set of model examples based on the ensemble of damped harmonic oscillators (Lorentz dispersion model). The consistency of calculated and measured spectral characteristics, as well as the accuracy of spectra reconstruction, has been shown.

We have shown that the selectivity of the calculated transmittance spectra is greater compared to the recorded reflectance spectra for several substances. Experiments on determining the sensitivity of the method for the detection and identification of substances have been carried out. The value of 30 μg was obtained for acetylsalicylic acid. This result can be further improved by introducing the reference infrared channel to compensate for the laser power instability that is currently a major factor limiting the method's sensitivity. We have estimated that the sensitivity for the upgraded setup corresponds to the minimum detection limit of about 10 $\mu\mathrm{g/cm}^2$ at a distance of about 1 m.

The design of the proposed experimental setup allows creating compact portable devices capable of real-time detection of substances on various surfaces. At the same time, the proposed method can be used in routine laboratory studies to complement the ATR and DRIFTS methods of IR spectroscopy.

Acknowledgments

The work was done at the department of physics of Bauman Moscow State Technical University in cooperation with the scientific-educational center "Photonics and IR-technology." The authors thank Professor Karasik, doctor of physics and mathematics, who made a huge contribution to the establishment and development of IR technology at Bauman Moscow State Technical University. The reported study was funded by RFBR according to the research project No. 18-29-02024 and by DAAD and Russian Ministry of Education according to the research project Michael Lomonosov Programm–Linie B, 2019 (57447934). The authors have no relevant financial interests in this article and no potential conflicts of interest to disclose.

References

1. H. Lin et al., "Methane detection using scattering material as the gas cell," *Appl. Opt.* **55**(28), 8030–8034 (2016).
2. M. Köhler et al., "Gas measurement using static Fourier transform infrared spectrometers," *Sensors* **17**, 2612 (2017).
3. K. V. Glagolev et al., "Technique for obtaining and processing spectral information with static Fourier spectrometer," *Opt. Spectrosc.* **110**(3), 449–455 (2011).
4. A. Goyal et al., "Detection of chemical clouds using widely tunable quantum cascade lasers," *Proc. SPIE* **9455**, 94550L (2015).

5. A. Morozov and S. Svetlichnyi, *Osnovy Fur'e-spektroradiometrii*, 2nd ed., Nauka, Moskva (2014).
6. B. Hapke, *Theory of Reflectance and Emittance Spectroscopy*, 2nd ed., Cambridge University Press, Cambridge (2012).
7. R. J. Bell, *Introductory Fourier Transform Spectroscopy*, Academic Press, New York (1972).
8. A. N. Morozov et al., "Physical principles of the design of an interferometer with a rotating plate," *J. Opt. Technol.* **80**(8), 495–498 (2013).
9. X. Tan et al., "Narrowband plasmonic metamaterial absorber integrated pyroelectric detectors towards infrared gas sensing," *Proc. SPIE* **10536**, 105361H (2018).
10. N. Vasil'ev et al., "Recovery and analysis of Raman spectra obtained using a static Fourier transform spectrometer," *Comput. Opt.* **41**(5), 626–635 (2017).
11. S. D. Christesen et al., "Handheld dual-wavelength Raman instrument for the detection of chemical agents and explosives," *Opt. Eng.* **55**(7), 074103 (2016).
12. L. Qiao et al., "Identification and quantitative analysis of chemical compounds based on multiscale linear fitting of terahertz spectra," *Opt. Eng.* **53**, 074102 (2014).
13. N. S. Vasil'ev, I. S. Golyak, and A. N. Morozov, "An algorithm for identification of substances using a finite set of secondary-emission spectra," *Opt. Spectrosc.* **118**(1), 151–156 (2015).
14. S. V. Bashkin et al., "Calculation of instrumental functions as a method for analyzing the alignment of the IR channel of a scanning Fourier-transform IR spectroradiometer," *Opt. Spectrosc.* **123**(4), 658–663 (2017).
15. A. N. Morozov, I. V. Kochikov, and I. L. Fufurin, "Numerical procedures for substances identification and concentration calculation in the open atmosphere by processing a single FTIR measurement," *Comput. Opt.* **36**(4), 554–561 (2012).
16. A. N. Morozov, S. I. Svetlichnyi, and I. L. Fufurin, "Correction of wavenumbers in a FTIR imaging spectrometer," *Doklady Phys.* **60**(9), 388–391 (2015).
17. S. V. Bashkin et al., "An imaging Fourier transform spectroradiometer with a multi-element photodetector for the spectral range of $7-14$ μm," *Opt. Spectrosc.* **121**(3), 449–454 (2016).
18. R. Harig and G. Matz, "Toxic cloud imaging by infrared spectrometry: a scanning FTIR system for identification and visualization," *Field Anal. Chem. Technol.* **5**(1-2), 75–90 (2001).
19. A. Portnov, S. Rosenwaks, and I. Bar, "Detection of particles of explosives via backward coherent anti-stokes Raman spectroscopy," *Appl. Phys. Lett.* **93**(4), 041115 (2008).
20. V. S. Gorelik et al., "Raman scattering in three-dimensional photonic crystals," *J. Russ. Laser Res.* **26**(3), 211–227 (2005).
21. T. S. Robinson and W. C. Price, "The determination of infra-red absorption spectra from reflection measurements," *Proc. Phys. Soc. Sec. B* **66**(11), 969–974 (1953).
22. E. R. Deutsch et al., "Active and passive infrared spectroscopy for the detection of environmental threats," *Proc. SPIE* **9106**, 91060A (2014).
23. J. A. Bardwell and M. J. Dignam, "Extensions of the Kramers–Kronig transformation that cover a wide range of practical spectroscopic applications," *J. Chem. Phys.* **83**(11), 5468–5478 (1985).
24. J. L. Musfeldt, D. B. Tanner, and A. J. Paine, "Method for the determination of the optical properties of highly conjugated pigments," *J. Opt. Soc. Am. A* **10**(12), 2648–2657 (1993).
25. R. H. Young, "Validity of the Kramers-Kronig transformation used in reflection spectroscopy," *J. Opt. Soc. Am.* **67**, 520–523 (1977).
26. I. S. Golyak et al., "Identification of chemical compounds by the reflected spectra in the range of $5.3-12.8$ μm using a tunable quantum cascade laser," *Russ. J. Phys. Chem. B* **13**(4), 557–564 (2019).
27. D. A. Samsonov, A. S. Tabalina, and I. L. Fufurin, "QCL spectroscopy combined with the least squares method for substance analysis," *J. Phys.: Conf. Ser.* **918**, 012034 (2017).
28. J. A. Lercher and A. Jentys, "Chapter 13 - Infrared and Raman spectroscopy for characterizing zeolites," in *Introduction to Zeolite Science and Practice*, J. Čejka et al., Eds., Studies in Surface Science and Catalysis, vol. **168**, pp. 435–476, Elsevier, Amsterdam (2007).
29. J. Lucas et al., "A fast Fourier transform implementation of the Kramers-Kronig relations: application to anomalous and left handed propagation," *AIP Adv.* **2**, 032144 (2012).

30. K. Ohta and H. Ishida, "Comparison among several numerical integration methods for Kramers–Kronig transformation," *Appl. Spectrosc.* **42**(6), 952–957 (1988).
31. C. W. Peterson and B. W. Knight, "Causality calculations in the time domain: an efficient alternative to the Kramers–Kronig method," *J. Opt. Soc. Am.* **63**(10), 1238–1242 (1973).
32. D. Roessler, "Kramers–Kronig analysis of reflection data," *Br. J. Appl. Phys.* **16**, 1119–1123 (2002).
33. S. S. Ng, Z. Hassan, and H. Abu Hassan, "Kramers–Kronig analysis of infrared reflectance spectra with a single resonance," *J. Teknologi* **44**(1), 67–76 (2006).
34. G. Andermann and L. R. Brantley, "Cauchy analysis of imaginary-dielectric-index bands," *J. Opt. Soc. Am.* **58**(2), 171–174 (1968).

Igor L. Fufurin is an associated professor in the chair of physics of the Bauman Moscow State Technical University. He received his BS and MS degrees in technical physics from the BMSTU in 2003 and 2007, respectively, and his PhD in optics from the BMSTU in 2011. He authored over 60 publications and 3 inventions. His scientific interests include atmospheric optics, spectroscopy, and calculus mathematics.

Anastasiia S. Tabalina is a student of MS degree at the Bauman Moscow State Technical University. She received her BS degree in physics from the BMSTU in 2018. Currently, she works as an engineer in the Research Department of JSC, "Center for Applied Physics BMSTU." She is also an executor of several grants of the Russian Foundation for Basic Research. She works in the field of IR spectroscopy and breath analysis.

Andrey N. Morozov is the doctor of physics and mathematics, professor, head of the Department of Physics, Deputy Director for Research, Scientific and Technological Center for Unique Instrumentation RAS, general director of the Center for Applied Physics, MSTU N.E. Bauman, honorary worker of Higher Professional Education of the Russian Federation. He is the author of over 280 scientific articles and 19 inventions. He published nine monographs and three textbooks. The main scientific works of A.N. Morozov devoted to the development of the theory and the creation of systems for passive optical location of chemical compounds in an open atmosphere, optoelectronic information-measuring systems, a description of irreversible and stochastic processes in precision measuring systems and control systems, and development of the theory of non-Markov random processes.

Igor S. Golyak is an associate professor in the chair of physics of the Bauman Moscow State Technical University. He received his BS and MS degrees in technical physics from the BMSTU in 2004 and 2008, respectively, and his PhD in mathematical modeling, numerical methods, and program complexes from the BMSTU in 2015. He authored over 50 publications. His scientific interests include spectroscopy and digital image processing.

Sergey I. Svetlichnyi successfully graduated from the Moscow Institute of Physics and Technology (MIPT) at the Faculty of Molecular and Chemical Physics in 1973. Now, he is working in Chernogolovka Branch of the N.N. Semenov Federal Research Center for Chemical Physics, Russian Academy of Sciences [FRCCP RAS (Chernogolovka)]. He holds a position of the leading researcher and candidate of physical and mathematical sciences. He is the author of 3 monographs and more than 100 publications in the field of chemical physics. His research interests are chemical lasers and IR spectroradiometry, including laser and Fourier spectrometers.

Dmitry R. Anfimov is a graduate student in the BMSTU Department of Physics. He received his BS degree in 2018. He works as an engineer at the Center for Applied Physics, BMSTU. He is the executor of several grants of the Russian Foundation for Basic Research.

Igor V. Kochikov is a leading researcher in the Research Computer Center of Moscow University. He has received doctoral degree in mathematical modeling, numerical methods and program complexes in 2003. He is the author of 162 articles and 6 books. His scientific interests include computational electrodynamics, molecular structure research, pattern recognition, and image processing.